Spherical SWE in GeoClaw

Working Notes, 27 October 2023

R. J. LeVeque

1 Background

The GeoClaw software (www.geoclaw.org, distributed as part of Clawpack [3]) is frequently used for modeling tsunamis and other wave propagation problems using the shallow water equations on a global scale. The equations are solved on rectagular grid patches in longitude-latitude space, and were implemented in a manner that deals with the varying finite volume grid cell sizes, which decrease when moving away from the equator and toward the poles.

Recently it was observed that the implementation does not fully implement the spherical coordinate form of the shallow water equations. In particular, a term is missing in the mass equation that can lead to waves decaying more than they should when propagating the poles, and less than they should when propagating toward the equator. Terms were also missing in the momentum equations, but these are quadratic in the fluid velocities and hence negligible for most realistic tsunami propagation problems, in which the depth-averaged fluid velocities are typically very small in the deep ocean where long-distance propagtion takes place.

Corrections have recently been incorporated into GeoClaw, which can be optionally invoked in Version 5.9.1 for testing purposes. The intention is to turn on at least the source term in the mass equation by default in future releases.

These notes further explain the issue and the correction terms and present the results of a number of test problems used to validate the new form, by comparing with fine-grid 1D solutions in the case of spherically symmetric test problems. We also explore the extent to which this correction changes the results of more realistic tsunami propagation problems. This is important in order to understand what error has been introduced in the past by the use of the incorrect equations in GeoClaw.

2 Notation

$$
\begin{aligned}
h &= \text{water depth in meters} \\
u, v &= \text{velocity in longitude,latitude directions, in m/s} \\
\lambda, \phi &= \text{longitude, latitude in radians} \\
x, y &= \text{longitude, latitude in degrees} \\
\gamma &= \pi/180 = \text{conversion factor from degrees to radians} \\
R &= \text{radius of the earth, in meters} \\
g &= \text{gravitational constant, in m/s}^2
\end{aligned}
$$

We explicitly include the conversion factor γ in formulas below for easier comparison with the GeoClaw code, in which γ is called `DEG2RAD`.

3 The 2D equations

The SWE in spherical coordinates on a constant-depth ocean (no bathymetry source terms) are often written in the form

$$h_t + \frac{1}{R\cos\phi}\left((hu)_\lambda + (hv\cos\phi)_\phi\right) = 0 \tag{1}$$

$$u_t + \frac{uu_\lambda}{R\cos\phi} + \frac{vu_\phi}{R} - \frac{uv\tan\phi}{R} + \frac{gh_\lambda}{R\cos\phi} = 0 \tag{2}$$

$$v_t + \frac{uv_\lambda}{R\cos\phi} + \frac{vv_\phi}{R} + \frac{u^2\tan\phi}{R} + \frac{gh_\phi}{R} = 0 \tag{3}$$

(omitting the Coriolis terms). This is the "advective form" given in [9] and derived, for example, in [5].

The mass equation (1) can be rewritten as:

$$h_t + \frac{(hu)_\lambda}{R\cos\phi} + \frac{(hv)_\phi}{R} = \frac{hv\tan\phi}{R}.$$

Converting from radians to degrees gives:

$$h_t + \frac{(hu)_x}{\gamma R\cos(\gamma y)} + \frac{(hv)_y}{\gamma R} = \frac{hv\tan(\gamma y)}{R}. \tag{4}$$

In GeoClaw a fractional step method can be used to handle the source term. Setting the right hand side to 0 and multiplying by $\gamma^2 R^2\cos(\gamma y)$ gives the equation

$$\gamma^2 R^2\cos(\gamma y)h_t + \gamma R(hu)_x + \gamma R\cos(\gamma y)(hv)_y = 0 \tag{5}$$

that is solved in the fractional step for the homogeneous shallow water equations in GeoClaw. Note that in this form, the factor $\gamma^2 R^2\cos(\gamma y)$ is the *capacity function*, the ratio of the area of a physical grid cell (in m^2) on the circle to $\Delta x\Delta y$ (in units of square degrees). The factors γR and $\gamma R\cos(\gamma y)$ multiplying the x- and y-derivatives in (5) are the length ratios of physical cell edge lengths to Δy and Δx respectively. (Note: In GeoClaw these length ratios multiply so-called f-waves, which are obtained by an eigendecomposition of the flux difference across each interface [1, 4]. Hence the metric term $\cos(\gamma y)$ is *outside* the y-derivatve in (5). If the length ratios multipied interface fluxes before flux differencing, then the metric term would be inside the y-derivative as in (1) and no source term would arise in this equation. This potential confusion could be at least partly responsible for the original omission of this source term in GeoClaw.)

The same GeoClaw Riemann solvers are used for both the 2D Cartesian and spherical cases, except for the addition of the length scale factors in the fluctuations returned. The capacity function is applied in the process of doing the flux differencing updates.

The source term in the mass equation (4) is currently omitted from GeoClaw. To properly incorporate the source term, the `src2.f90` routine should be modified to take a time step on

$$h_t = \frac{\tan(\gamma y)}{R}(hv).$$

Source terms are also needed in the momentum equations. The x-momentum equation (2) can be combined with the mass equation and massaged to obtain

$$(hu)_t + \frac{1}{\gamma R\cos(\gamma y)}\left(hu^2 + \frac{1}{2}gh^2\right)_x + \frac{1}{\gamma R}(huv)_y = \frac{2\tan(\gamma y)}{R}(huv). \tag{6}$$

GeoClaw solves the homogeneous version of this in the form

$$\gamma^2 R^2\cos(\gamma y)(hu)_t + \gamma R\left(hu^2 + \frac{1}{2}gh^2\right)_x + \gamma R\cos(\gamma y)(huv)_y = 0$$

with the same capacity and length ratio factors as in the mass equation. To add the source term, we need to take a time step on

$$(hu)_t = \frac{2\tan(\gamma y)}{R}(huv).$$

Finally, the y-momentum equation (3) can be combined with the mass equation and massaged to give

$$(hv)_t + \frac{1}{\gamma R\cos(\gamma y)}(huv)_x + \frac{1}{\gamma R}\left(hv^2 + \frac{1}{2}gh^2\right)_y = \frac{\tan(\gamma y)}{R}\left(hv^2 - hu^2\right). \tag{7}$$

GeoClaw solves the homogeneous version of this in the form

$$\gamma^2 R^2\cos(\gamma y)(hv)_t + \gamma R(huv)_x + \gamma R\cos(\gamma y)\left(hv^2 + \frac{1}{2}gh^2\right)_y = 0.$$

To add the source term, we need to take a step on

$$(hv)_t = \frac{\tan(\gamma y)}{R}\left(hv^2 - hu^2\right).$$

To summarize, the 2D shallow water equations are given by (4), (6), (7). These should agree with the "flux form" in [9].

4 GeoClaw modification in 2D

The `src2.f90` routine in GeoClaw has been modified by the addition of the loop shown in Figure 1. `coordinate_system == 2` means we are solving on the sphere in longitude-latitude coordinates. Setting `sphere_source == 0` omits the source terms for backward compabtibility. Setting `sphere_source == 1` includes only the source term in the mass equation for `q(1,i,j)`, which is the most critical one to include. Setting `sphere_source == 2` also includes the source terms in the momentum equations. These are quadratic in velocities (which are small in the deep ocean) and can probably be dropped for most practical problems. See Section 10 for more discussion.

```
if ((coordinate_system == 2) .and. (sphere_source > 0)) then
    ! add in spherical source term in mass equation
    ! if sphere_source in [1,2],
    ! and also in momentum equations if sphere_source == 2
    do j=1,my
        y = ylower + (j - 0.5d0) * dy
        tanyR = tan(y*DEG2RAD) / earth_radius
        do i=1,mx
            if (q(1,i,j) > dry_tolerance) then
                ! source term in mass equation:
                q(1,i,j) = q(1,i,j) + dt * tanyR * q(3,i,j)

                if (sphere_source == 2) then
                    ! Momentum source terms that drop out if linearized:
                    ! These seem to have very little effect for
                    ! practical problems
                    huv = q(2,i,j)*q(3,i,j)/q(1,i,j)
                    huu = q(2,i,j)*q(2,i,j)/q(1,i,j)
                    hvv = q(3,i,j)*q(3,i,j)/q(1,i,j)
                    q(2,i,j) = q(2,i,j) + dt * tanyR * 2.d0*huv
                    q(3,i,j) = q(3,i,j) + dt * tanyR * (hvv - huu)
                endif
            endif
        enddo
    enddo
```

Figure 1: Proposed modification to the GeoClaw Fortran subroutine `$CLAW/geoclaw/src/2d/shallow/src2.f90`. The full routine can be viewed in Github at https://github.com/clawpack/geoclaw/blob/master/src/2d/shallow/src2.f90.

5 Axisymmetric solutions, 1D equations

If the initial data is a function of latitude alone then the solution remains axisymmetric and the equations (4) for mass and (7) for the y-momentum reduce to the one-dimensional system of equations

$$h_t + \frac{1}{\gamma R}(hv)_y = \frac{\tan(\gamma y)}{R}(hv) \tag{8}$$

$$(hv)_t + \frac{1}{\gamma R}\left(hv^2 + \frac{1}{2}gh^2\right)_y = \frac{\tan(\gamma y)}{R}\left(hv^2\right). \tag{9}$$

In the 1D GeoClaw code, these are solved by alternating between a hyperbolic step with the 1D shallow water equations with the addition of a capacity function γR,

$$\gamma R\, h_t + (hv)_y = 0, \tag{10}$$

$$\gamma R\,(hv)_t + \left(hv^2 + \frac{1}{2}gh^2\right)_y = 0, \tag{11}$$

and a source term time step on

$$h_t = \frac{\tan(\gamma y)}{R}(hv), \tag{12}$$

$$(hv)_t = \frac{\tan(\gamma y)}{R}\left(hv^2\right). \tag{13}$$

Note that near each pole the axisymmetric equations (8) and (9) reduce to the 1D planar equations with radial symmetry. Near the south pole, $y \approx -90$, $\gamma y \approx -\pi/2$, the radial distance from the pole is roughly

$$r = R(\gamma y + \pi/2).$$

In this case $dr/dy = \gamma R$ and

$$\tan(\gamma y) = \frac{\sin(\gamma y)}{\cos(\gamma y))} \approx \frac{-1}{\gamma y + \pi/2} = -\frac{R}{r},$$

so the equations (8), (9) reduce to

$$h_t + (hv)_r = -\frac{1}{r}(hv) \tag{14}$$

$$(hv)_t + \left(hv^2 + \frac{1}{2}gh^2\right)_r = -\frac{1}{r}\left(hv^2\right). \tag{15}$$

These are the standard radial equations. Similarly, near the north pole set $r = R(\pi/2 - \gamma y)$ and note that v must also be negated (since positive v in the spherical case corresponds to flow toward the pole) to derive the same radial equations.

6 Verification tests

A simple axisymmetric test is to start with a hump of water on a ring around the sphere at some latitude, giving rise to waves propagating both north and south. Figure 2 shows results of how this evolves in time for the case where the ring is at the equator $y = 0$. The left column shows results with the proper spherical source terms included and gives the behavior that should be expected due to conservation of mass: as the wave moves towards the poles it increases in amplitude since the total mass of the hump around the sphere is the mass in this cross section multiplied by a circumference that decreases as the cosine of the latitude.

The right column shows the results with the 1d code if the source terms are omitted. The 1d equations are just a scaled version of the 1d SWE for a planar wave and so, after splitting apart, the waves propagate with no change in amplitude as they approach the poles (until the final time shown, when they reflect due to the solid wall boundary conditions at these boundaries).

Solving the 2D equations with GeoClaw v5.9.0 (which lacks the spherical source term) for the same range of latitudes and a very coarse grid in the longitude direction for $-10 \leq x \leq 10$ gives results that are essentially identical to the right column. Modifying the code by including the source terms indicated above gives results equivalent to the left column. This indicates that the source terms should indeed be added to GeoClaw.

Note that when the 2D GeoClaw code is run with initial data that is axisymmetric and varies only with y, all of the x-derivative terms and those involving the u velocity drop out, so the code reduces to solving the 1D equations. So it is not surprising that the 1D and 2D results agree very well in each case (with or without source terms) because we are using longitude-latitude coordinates in 2D. Hence this agreement does not necessarily mean that the source terms added are correct in either case, although the behavior looks more physically correct. It also does not verify that the 2D source terms that depend on x or u are correct since these drop out with axisymmetric data.

A better comparison test is to perform an experiment in which the initial data is again an axisymmetric ring, but about an axis that is not the polar axis of the earth. As an example, we take an axis that goes through the equatorial points $(0, 0)$ and $(180, 0)$ with a ring of elevated surface elevation that is 20 degrees away these points as shown in Figure 3 in longitude-latitude space. This figure also shows a scatter plot of the surface η vs. great circle distance from (0,0) for all 2D finite volume cells. For this initial data these points should all lie on a curve with the peak at a distance of roughly 222 km ($= 20\gamma R$ in our notation). This initial data results in two waves, one moving inwards toward (0,0) and the other moving outwards. This solution should always remain axisymmetric about the axis through (0,0), and so a similar scatter plot of the solution should always give the points lying nearly on a curve that agrees with a 1D solution. We see this expected behavior in the top plots of Figure 4, where GeoClaw with the addition of the spherical source terms was used to solve the problem (in the usual x-y coordinates, so the 2D code is not reducing to solving 1D equations in this case). Note that in the x-y plane the outgoing ring does not look circular, but it would if plotted on the sphere. Contours of η are also shown, from which it is also clear that the peak amplitude is roughly constant as one goes around the ring.

By contrast, the bottom figures of Figure 4 show the solution obtained with GeoClaw v5.9.0, without the spherical source terms. The outgoing wave does not have constant amplitude as one goes around the ring, as clear both from the contour plot and from the scatter plot. The

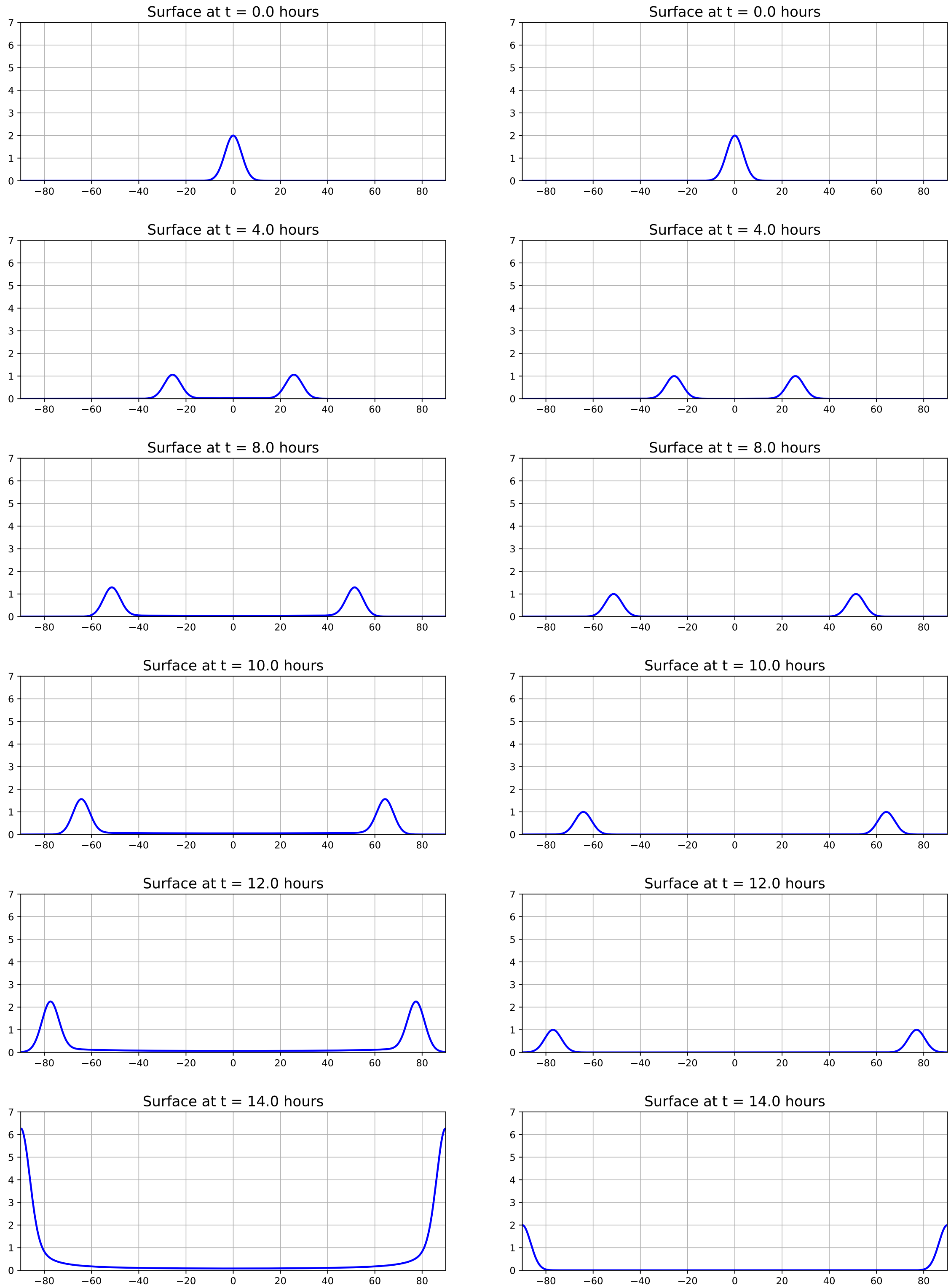

Figure 2: One-dimensional test with an axisymmetric ring of water around the equator as initial conditions, giving waves moving north and south. The simulations are the left are with the proper source term added, those on the right lack the spherical source term.

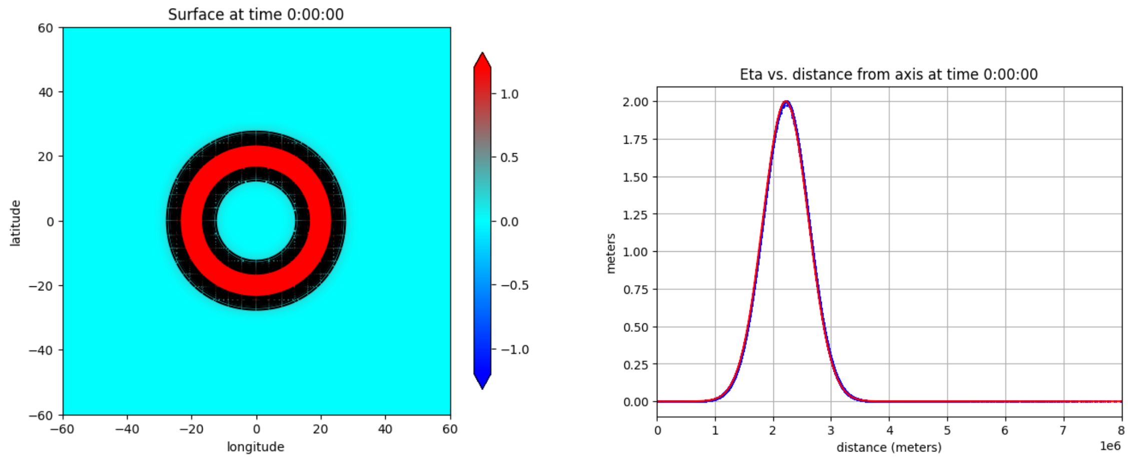

Figure 3: Initial data for GeoClaw axisymmetric test with nonpolar axis through (0,0). Left: in Longitude-Latitude space, with contours at $\eta = 0.2,\ 0.3,\ \ldots,\ 1.2$. Right: Scatter plot of surface η vs. radial distance from (0,0).

upper envelope of the scatter plot agrees well with the solution from Figure 4 (and presumably with the 1D solution). These points where the amplitude is nearly correct lie on the equator $y = 0$. The waves propagating in this direction are nearly correct because the $\tan(\gamma y)$ source terms vanish at $y = 0$. The waves propagating due north or south along $x = 0$ are the ones that have the smallest amplitude. This make sense since the source terms amplify waves moving towards the pole, so leaving them out results in waves that are too small. We see a significant underprediction for waves traveling from 20°N to 52°N in this case. Note that this is roughly the latitude difference between Hawaii and Aleutian Islands, although for the case of a tsunami generated in Alaska and traveling south, the error from omitting the source terms should result in an *overprediction* of the wave height, rather than an underprediction, so at least for this important scenario the version of GeoClaw in use now should be overly conservative. This is explored further in the next section.

7 Test on a Hypothetical AASZ Tsunami

To see what effect this source term has on a more realistic tsunami, we consider a hypothetical earthquake on the Aleutian-Alaska Subduction Zone that generates a large tsunami directed towards Hawaii, as developed by Butler et al. [2].

Figure 5 shows the simulated tsunami at 1,3, and 5 hours, both when the spherical source terms are add (on the left) and without those terms (on the right). The wave pattern are nearly identical, only the magnitude changes, and as expected adding the source terms slightly reduces the magnitude of the wave traveling towards the equator.

This can be seen better in the transect plots shown on Figure 6, which shows a cross section of the ocean surface along the transect shown in Figure 5 at 1,2,3,4, and 5 hours, for both simulations. Again note that the wave patterns and timing are almost identical, but there is a difference in amplitude of up to 20%.

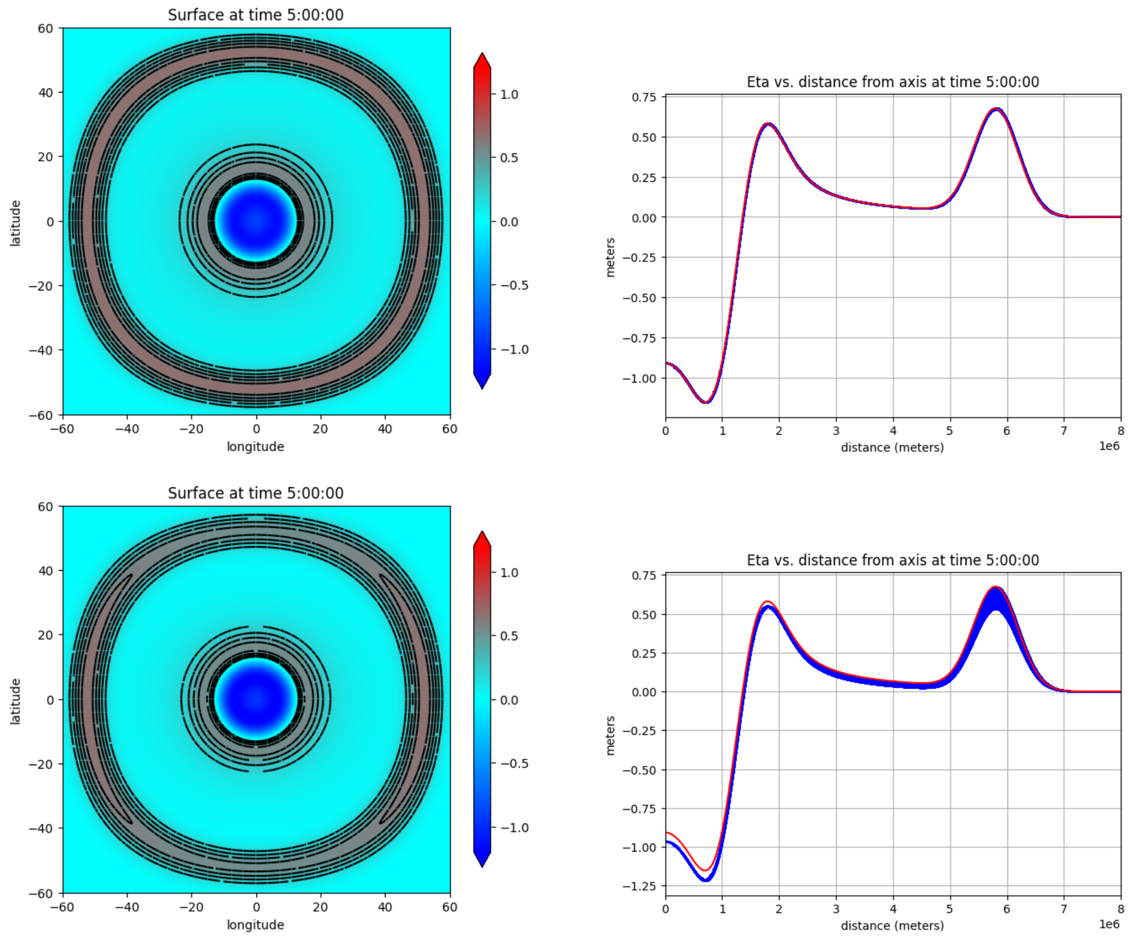

Figure 4: GeoClaw solution at $t = 5$ hours when spherical source terms are included (on top) and without these terms (on bottom). Plots on the left again have contours at $\eta = 0.2,\ 0.3,\ \ldots,\ 1.2$. Plots on the right show scatter plots of the 2D solution (blue dots) together with the 1D axisymmetric solution computed on a very fine grid (red curve). Note that the amplitude of the outgoing waves are nearly constant in all directions only when the source terms are included.

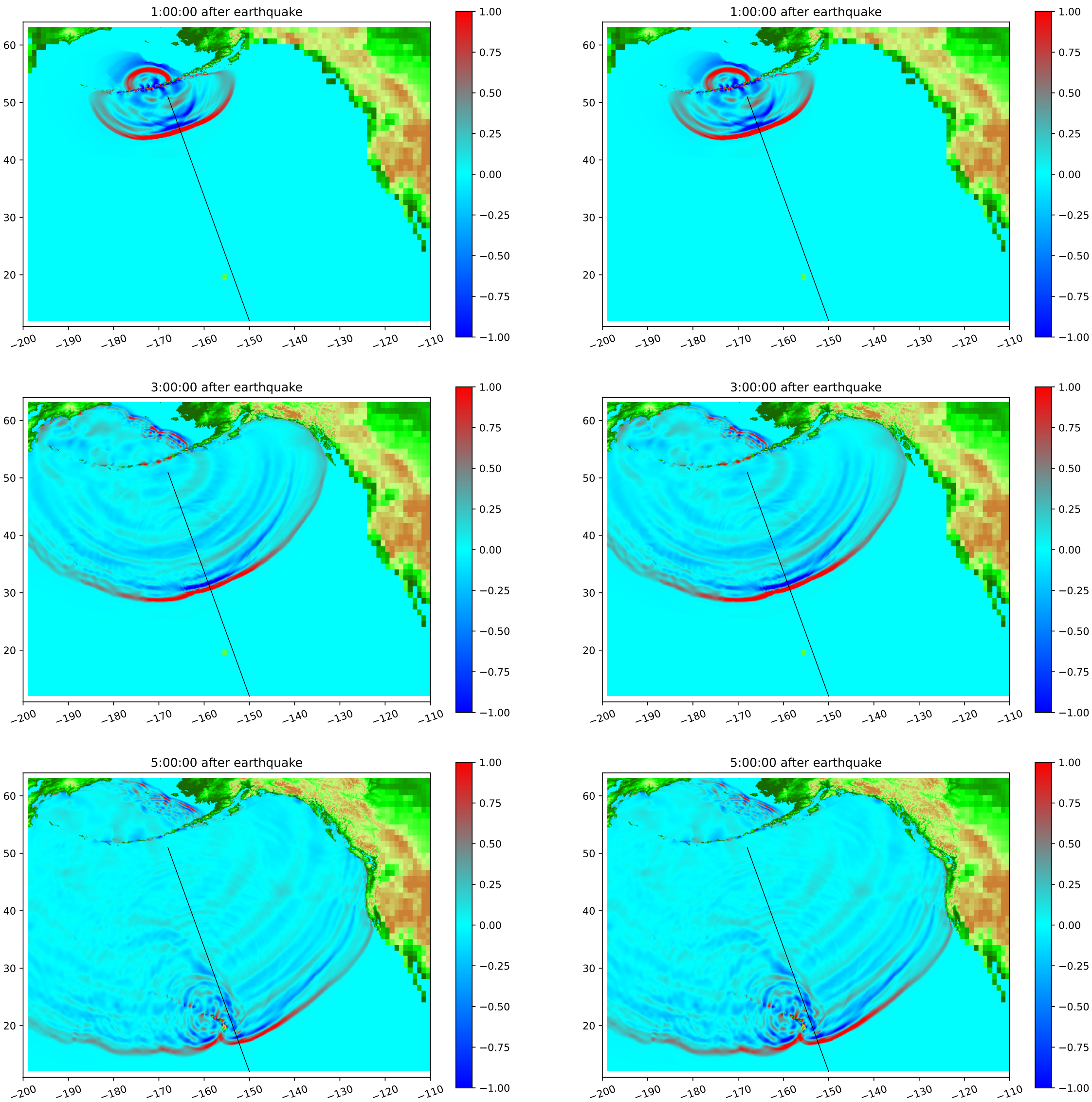

Figure 5: AASZ tsunami simulation with source terms included (left) and with GeoClaw 5.9.0 (right). The wave pattern are nearly identical, only the magnitude changes slightly.

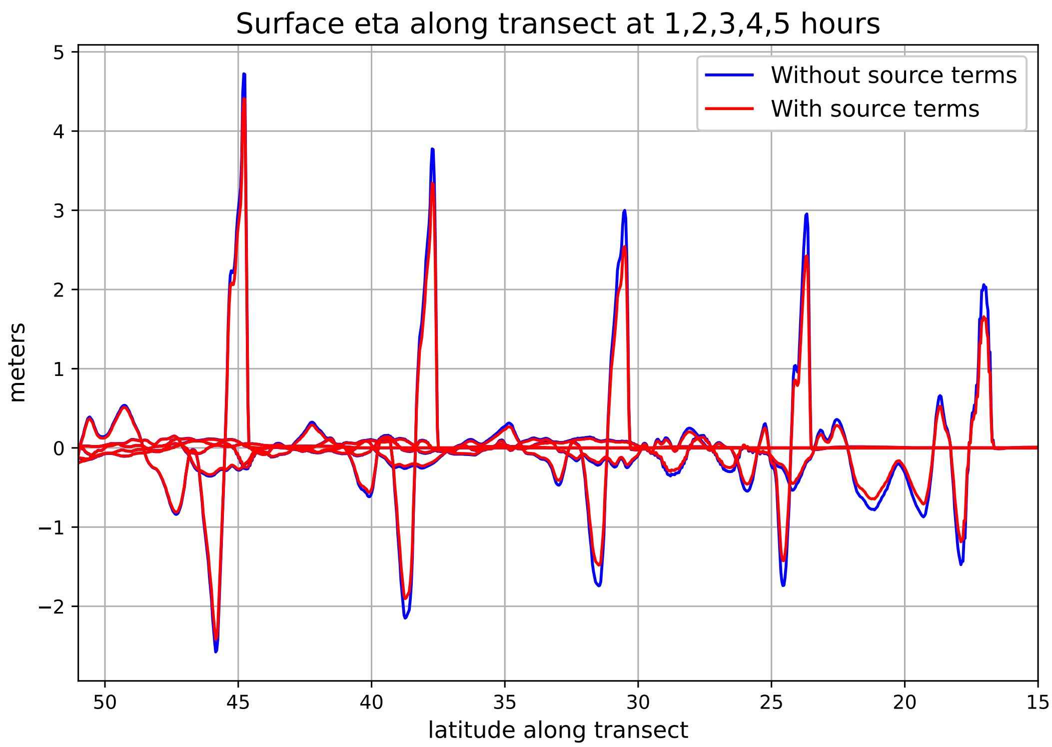

Figure 6: Transect of the surface elevation along the transect shown in Figure 5, at 1,2,3,4, and 5 hours.

8 Test on the 2011 Tohoku Tsunami

Figures 7 and 8 show a similar experiment for the Tohoku Japan 2011 event. The plots shown in Figure 7 are for the case with the spherical source terms included but for this event they look nearly indistinguishable from those without the source terms, particularly for the wave propagating towards Hawaii along the transect indicated, at relatively constant latitude. Figure 8 shows the surface along this transect at 1–6 hours, and in this case there is little difference in the amplitude.

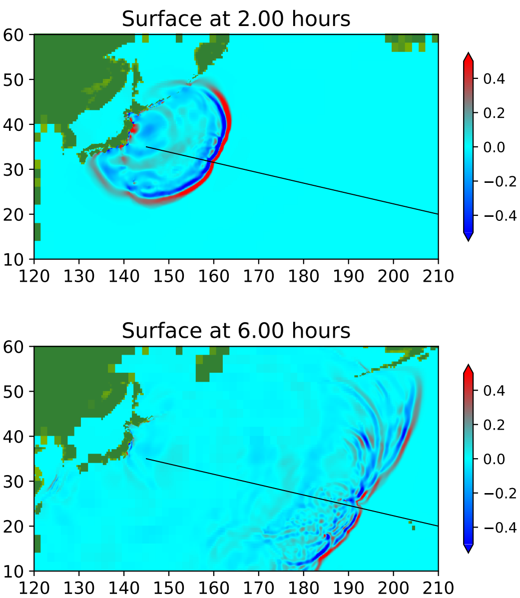

Figure 7: Tohoku Japan 2011 tsunami simulation at 2, 4, 6, and 8 hours (with spherical source terms included.

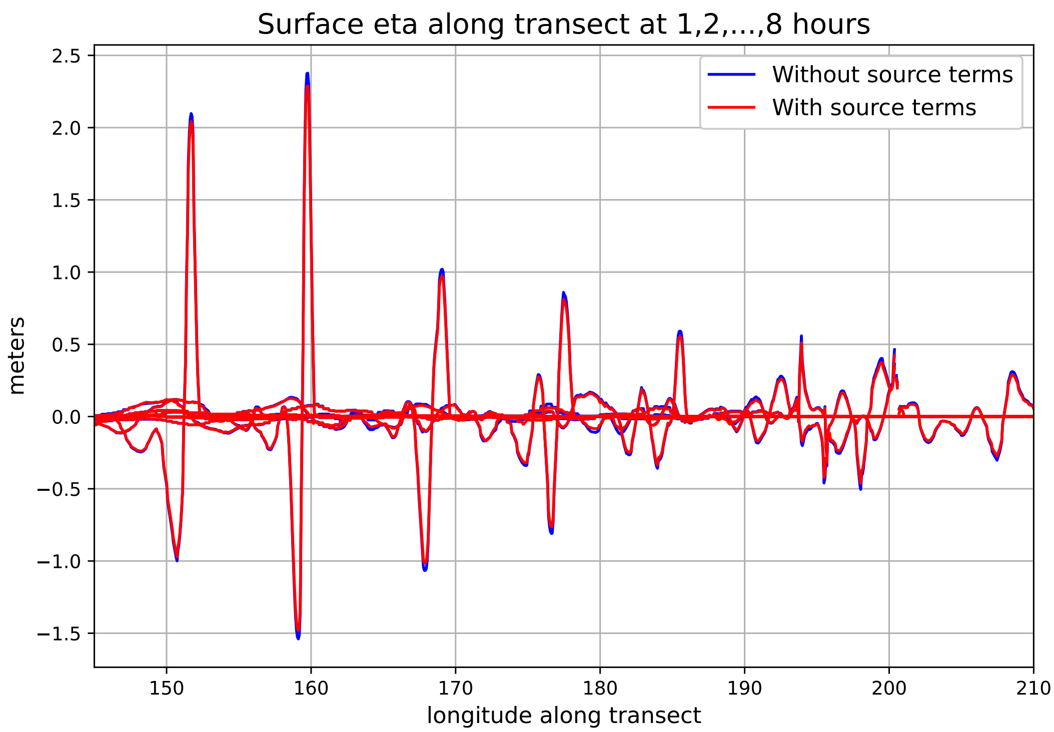

Figure 8: Transect of the surface elevation along the transect shown in Figure 7, at $t = 1,\ 2,\ \ldots,\ 8$ hours.

9 Conservation of mass

In principle the shallow water equations should conserve mass on the sphere. (For problems with onshore inundation we don't expect conservation if the AMR levels change near the coast during inundation, but for a pure ocean problem we should hope for exact conservation even when AMR is used.)

In the 1D PDEs (8) and (9), conservation of mass can be verified by noting that each value $h(y, t)$ represents a band of water around a circle of radius $2\pi R\cos(\gamma y)$ at this latitude, so the total mass on the surface of the sphere is

$$\int_{-90}^{90} 2\pi R\cos(\gamma y)h(y,t)\,dy$$

Taking the time derivative of this, and moving it inside and then replacing h_t using (8), we obtain

$$\frac{d}{dt}\int_{-90}^{90} 2\pi R\cos(\gamma y)h(y,t)\,dy = \int_{-90}^{90} 2\pi R\cos(\gamma y)\left(-\frac{1}{\gamma R}(hv)_y + \frac{1}{R}\tan\gamma y(hv)\right)dy \tag{16}$$

$$= -\frac{2\pi}{\gamma}\int \cos(\gamma y)(hv)_y\,dy + 2\pi\int \sin(\gamma y)\,(hv)\,dy. \tag{17}$$

Integrating by parts in the first integral gives a new integral that cancels out the second integral above, leaving only the boundary term

$$\frac{d}{dt}\int_{-90}^{90} 2\pi R\cos(\gamma y)h(y,t)\,dy = -\frac{2\pi}{\gamma}(hv)\cos(\gamma y)\Big|_{-90}^{90} \tag{18}$$

$$= 0, \tag{19}$$

giving conservation.

For the 1D numerical solution, each cell average value H_i^n represents the average solution in a band around the sphere from latitude $y_{i-1/2}$ to $y_{i+1/2}$. The width of this band in meters is $\gamma R\Delta y$, and each circle in the band has length $2\pi R\cos(\gamma y)$, so the total area of the band is

$$2\pi\gamma R^2\int_{y_{i-1/2}}^{y_{i+1/2}} \cos(\gamma y)\,dy = 2\pi R^2\left(\sin(\gamma y_{i+1/2}) - \sin(\gamma y_{i-1/2})\right).$$

(Note that summing this over all bands between $y = \pm 90$ gives $4\pi R^2$, the surface area of the full sphere.)

So to compute the discrete mass corresponding to the finite volume solution H_i^n, we should multiply each depth value by the area of the corresponding band to compute the discrete volume:

$$\text{Total mass at time } t_n = \sum_i 2\pi R^2\left(\sin(\gamma y_{i+1/2}) - \sin(\gamma y_{i-1/2})\right)H_i^n.$$

Should we expect this to be conserved? I don't think so, even if the correct source terms are included. The proof of conservation in the PDE above requires exact cancellation of the the source term with the term that arises from integration by parts. If we use a fractional step method in GeoClaw to add in the source term, then it is calculated based on the result of first taking a step with the SWE, and it seems that any such exact cancellation would be impossible. Perhaps the source term can be incorporated more directly into the SWE time step (similar to how the topography source term much be incorporated into the Riemann solver in order to maintain conservation on non-flat topography in the Cartesian case). This seems more complicated, but I haven't examined it in detail yet.

At least it is true that mass is much better conserved with the source term than without. Figure 9 shows the total mass as formulated above for the 1D results presented in Figure 2. This actually shows the relative change in the mass of the wave, not the underlying water. Since the ocean was 4000 m deep everywhere while the wave has an amplitude of a few meters, the mass of the wave (and any errors in it) would be overwhelmed by the mass of the ocean otherwise. Figure 10 shows a similar plot for the simulation shown in Figure 3, again for the mass in the wave alone. After $t = 5$ hours the waves reach the extrapolation boundaries and conservation would not be expected.

10 Linearizations

When linearizing the SWE about an ocean at rest we drop all terms that are quadratic in velocities. Then the 2D spherical equations (1–3) in advective form become

$$h_t + \frac{1}{R\cos\phi}\left((hu)_\lambda + (hv\cos\phi)_\phi\right) = 0 \tag{20}$$

$$u_t + \frac{gh_\lambda}{R\cos\phi} = 0 \tag{21}$$

$$v_t + \frac{gh_\phi}{R\cos\phi} = 0 \tag{22}$$

The spherical source term in the mass equations remains but those in the velocity equations drop out. For tsunami propagation in the deep ocean these equations give solutions that agree very well with the full nonlinear equations. This suggests that even in the nonlinear equations one could drop the spherical source terms with little impact on the solution (because for long-distance propagation the tsunami is primarily in deep water, where the nonlinearities are unimportant, and near shore the nonlinearities are important but the propagation distances are short). In fact, some other tsunami models appear to drop the spherical source terms from the velocity (or momentum) equations even in their "nonlinear" form, e.g., the equations on p. 2 of [7], which describes the MOST model, equations (2.8)–(2.10) of the COMCOT User Manual [8], or equations (1)–(2) of [6], which describes the FUNWAVE-TVD model (these equations also include dispersive terms, which we omit here). Other tsunami models retain these terms, e.g. equations (4)–(6) of [10] describing NEOWAVE.

Repeating the test from Section 7 without the nonlinear spherical source terms in the momentum equations gives results that are identical to those shown in Figures 5 and 6 when all source terms are included. Leaving out the nonlinear source terms simplifies the GeoClaw modification given in Section 4 to only update `q(1,i,j)`.

As a test to show that the momentum source terms are correct in a case where they do matter, we perform a test similar to that shown in Figure 4, but in a case where the axis of symmetry cuts through the earth at latitude 60 so that there is considerable variation in latitude over the outgoing waves. Even so, with a realistic ocean depth there is virtually no difference in the resulting waves regardless of whether the source terms in momentum are included or not (provided the source terms in the mass are included, as seen in an experiment not shown

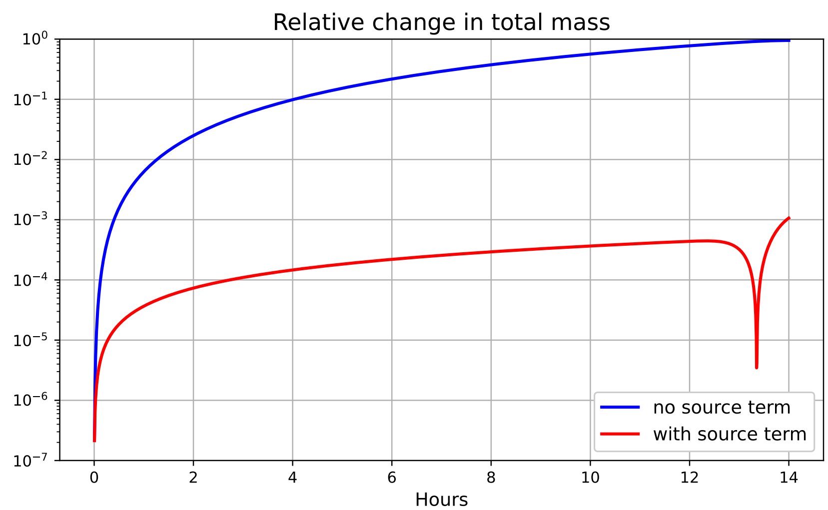

Figure 9: Total mass from the 1D simulations of Figure 2.

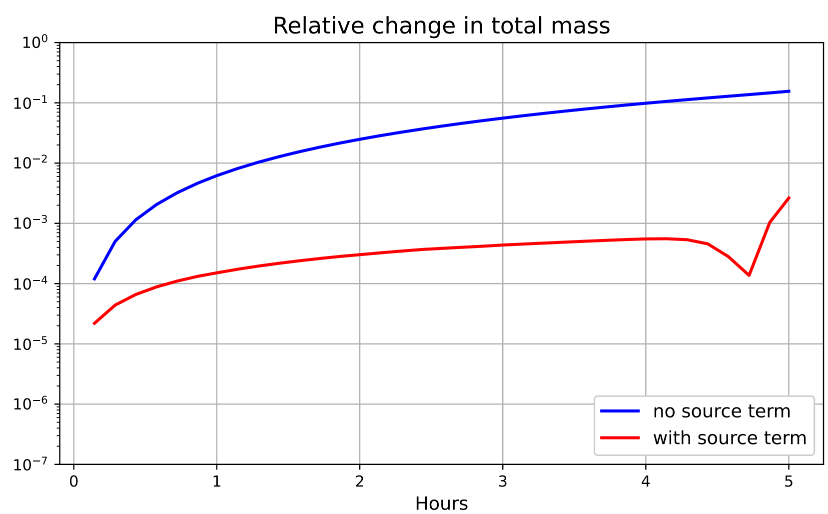

Figure 10: Total mass from the 2D simulations of Figure 3.

here). In order for these nonlinear terms to become important we consider a highly unrealistic case with an ocean of uniform depth 1 meter. As initial conditions we take a Gaussian hump centered at (0,60), with elevation 2m on top of the background depth of 1m. This gives an outgoing wave that steepens into a shock wave, and the nonlinear terms in the equations are non-negligible. Because the wave speed is small in this case the simulation is run out to 108 hours (4.5 days) in order for the wave to move out a comparable distance to that shown in the previous test. The radially expanding shock wave is shown in longitude-latitude coordinates in Figure 11. Figure 12 shows scatter plots of the elevation at this time as computed without the spherical source terms, with only the mass term, and when the momentum source terms are also included. In this case we see that the addition of the nonlinear momentum source terms decreases the scatter and improves the agreement with the 1-dimensional axi-symmetric solution shown as a red curve in each case.

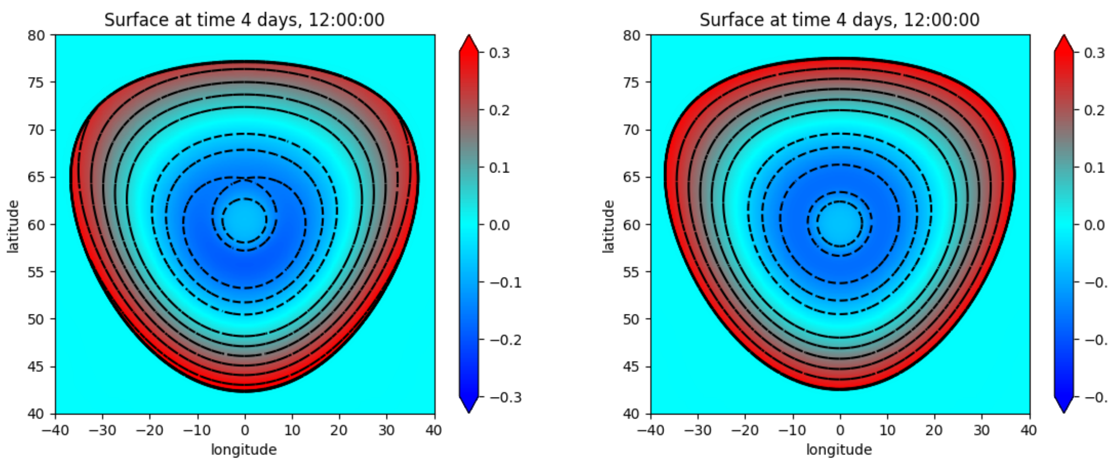

Figure 11: GeoClaw solution at $t = 108$ hours with an ocean of uniform depth 1 meter, and an initial hump of amplitude 2 meters centered at latitude 60. Left: without the spherical source terms. Right: with all spherical source terms. Contours are at $\pm 0.05, \ \pm 0.1, \ \ldots, \ \pm 0.3$ m elevation.

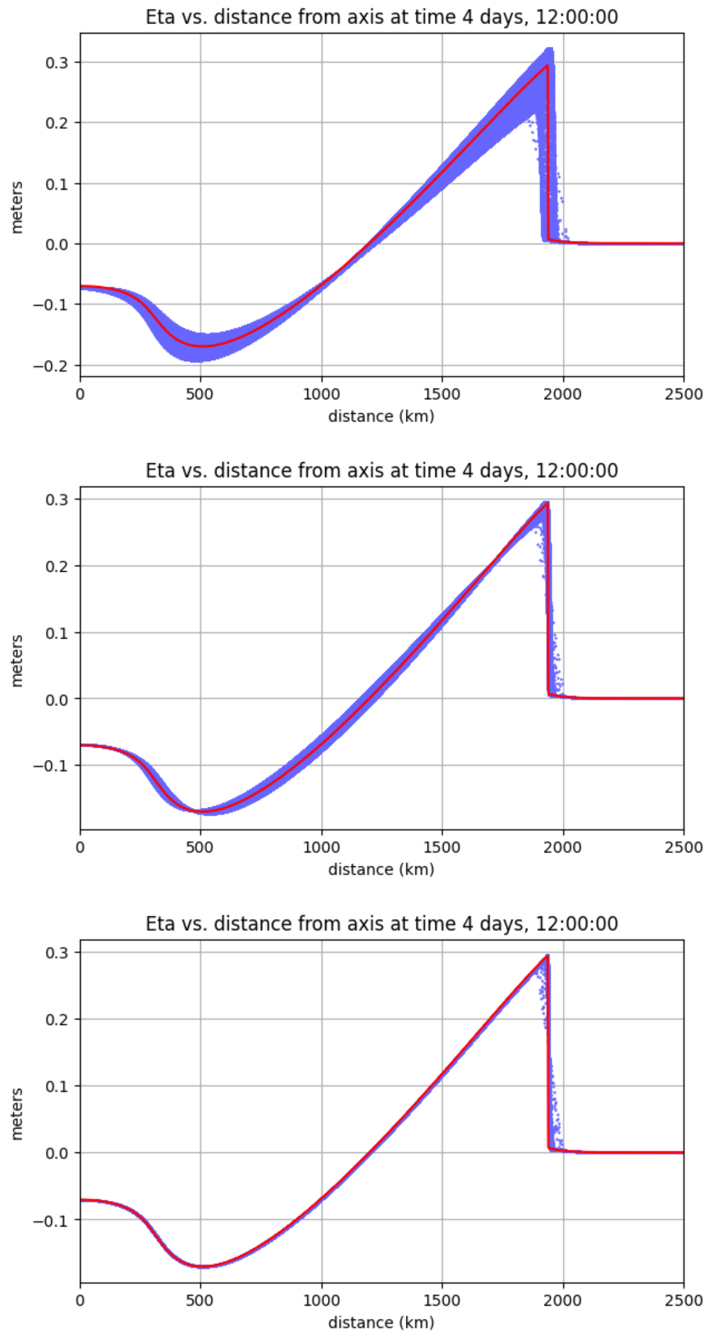

Figure 12: Scatter plots of the solution for the highly nonlinear problem shown in Figure 11 from simulations with (a) no spherical source terms, (b) only the source term in mass, (c) also the source terms in momentum. The red curve is the axisymmetric 1D solution computed on a fine grid.

References

[1] D. Bale, R. J. LeVeque, S. Mitran, and J. A. Rossmanith, *A wave-propagation method for conservation laws and balance laws with spatially varying flux functions*, SIAM J. Sci. Comput., 24 (2002), pp. 955–978.

[2] R. Butler, D. Walsh, and K. Richards, *Extreme tsunami inundation in Hawai'i from Aleutian–Alaska subduction zone earthquakes*, Nat Hazards, 85 (2017), pp. 1591–1619.

[3] Clawpack Development Team, *Clawpack software*.

[4] R. J. LeVeque, D. L. George, and M. J. Berger, *Tsunami modeling with adaptively refined finite volume methods*, Acta Numerica, (2011), pp. 211–289.

[5] D. Raymond, *Shallow water on a sphere*. Lecture Notes, http://kestrel.nmt.edu/~raymond/classes/ph332/notes/sphere/sphere.pdf, 2022.

[6] F. Shi, J. T. Kirby, and B. Tehranirad, *Tsunami benchmark results for spherical coordinate version of FUNWAVE-TVD*. https://www1.udel.edu/kirby/papers/shi-etal-cacr-11-02-version1.1.pdf, 2012.

[7] V. Titov and F. I. González, *Implementation and testing of the method of splitting tsunami (MOST) model*. NOAA Technical Memorandum ERL PMEL-112, https://repository.library.noaa.gov/view/noaa/10979, 1997.

[8] X. Wang, *COMCOT Users' Manual, v1.7*. https://github.com/efzyx/comcotpraba, 2009.

[9] D. L. Williamson, J. B. Drake, J. J. Hack, R. Jakob, and P. N. Swarztrauber, *A standard test set for numerical approximations to the shallow water equations in spherical geometry*, Journal of Computational Physics, 102 (1992), pp. 211–224.

[10] Y. Yamazaki, Y. Bai, L. L. Goo, K. F. Cheung, and T. Lay, *Nonhydrostatic modeling of tsunamis from earthquake rupture to coastal impact*, Journal of Hydraulic Engineering, 149 (2023), p. 04023033.